

# Hot corrosion of $\alpha$ -SiC ceramics by $V_2O_5$ melt

WEN C. SAY\*, JIANN K. WU, W. L. CHEN

Department of Materials Engineering, Tatung Institute of Technology, Taipei, Taiwan, 10451, Republic of China

The corrosion behaviour of  $\alpha$ -SiC in  $V_2O_5$  melt has been investigated at elevated temperatures. The corrosion products on the surface of the specimen are removed using HF. The morphologies are also examined. From the observations of bubble formation in the scale and the temperature dependence of the corrosion rate, a kinetic mechanism is proposed. Based on the consistency of the plotted data with the proposed equation and high values of surface reaction rate constant, a diffusion controlling process has been developed.

## 1. Introduction

Because of its low thermal expansion and high thermal conductivity silicon carbide (SiC) is an attractive material for gas turbine engines. Unfortunately, this material has been found disadvantageous because of its corrosive behaviour at elevated temperatures.

Many investigations have shown that SiC is corroded by molten salt [1-3]. Although the stable  $SiO_2$  layer is formed to protect the SiC from further dissolution, the basic melt will accelerate the corrosion rate by dissolving the oxidized layer. McKee and Chatterji [4] concluded that the SiC was passive in neutral or acid salt melts under the normal conditions. However, the present experiments show that  $V_2O_5$ , as a low melting point ( $658^\circ\text{C}$ ) acid salt, is still able to corrode SiC. It is known that vanadium-rich oil is found in certain wells in South America. The ash of such oils may reach 65%  $V_2O_5$  or higher, and the damage caused by the ash in engines is severe [5].

The purpose of this paper is to study the kinetic mechanism of the elevated temperature corrosion of sintered  $\alpha$ -SiC in molten  $V_2O_5$  acid salt.

## 2. Experiments

### 2.1. Materials

The material used was 4 g dense  $\alpha$ -SiC ceramic with added 2 wt% AlN. The hot-pressed billets from Hitachi [6] were cut into 1 mm thick blocks 25 mm  $\times$  25 mm and have a freshly polished surface for each experiment. Reagent grade  $V_2O_5$  (40 g) was used as the melting medium in the test. The cleaning solution was prepared by diluting 10% HF concentrate in deionized water.

### 2.2. Procedures

Silicon carbide and vanadium oxide were heated simultaneously at 700, 800, 900 and  $1000^\circ\text{C}$  respectively. Corrosion experiments were performed in a graphite crucible in which SiC specimen had been completely immersed in the  $V_2O_5$  melt at the desired temperatures

for up to 10 h. Oxide scales from each run of the corrosion tests were removed using a cleaning solution [3, 7]. Corrosion behaviour was studied by monitoring the specimen weight, which was measured in terms of weight change per unit area  $\Delta W/A$  ( $\text{cm}^2$ ). Meanwhile, an atomic absorption equipment (AA) was used to determine qualitatively the content of silicon, and scanning electron microscopy (SEM) was applied to examine the morphologies. Figure 1 is a flowsheet of the tests for each data point.

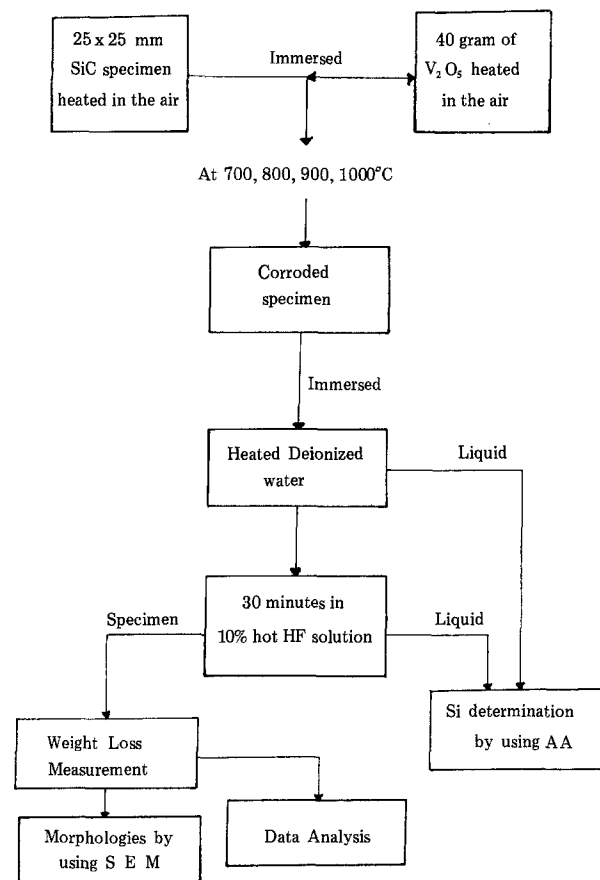


Figure 1 Schematic diagram of the experimental analysis for each data point.

\*Present address: Department of Materials and Mineral Resources Engineering, National Taipei Institute of Technology, Taipei, Taiwan 10626, Republic of China.

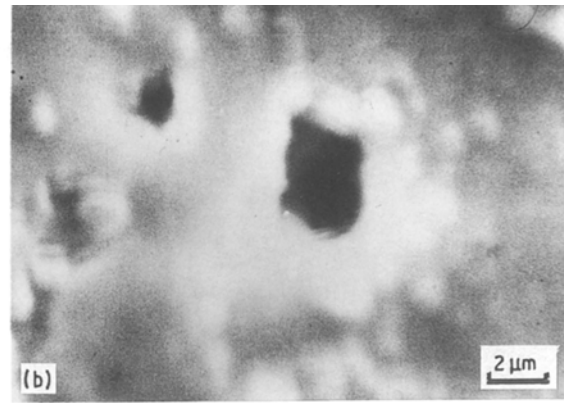
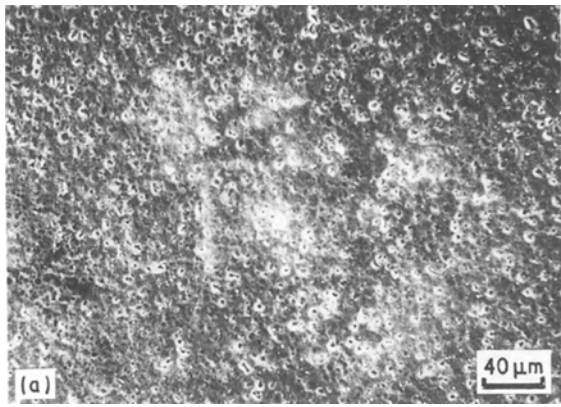
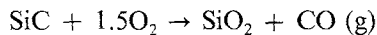


Figure 2 Morphology of the SiC surface after 10 h of  $V_2O_5$  corrosion at  $1000^\circ C$ . The scale has been removed by HF dissolution. The surface shows a coarse network of pits (a), and pits averaging  $2\text{--}3\ \mu\text{m}$  in diameter.

### 3. Results and discussion

The SiC morphology after 10 h in  $V_2O_5$  acid melt at  $1000^\circ C$  and after undergoing scale dissolution in HF solution is shown in Fig. 2. Figure 2a shows corrosion pits on the surface of the specimen. Figure 2b shows pits of on average  $2\text{--}3\ \mu\text{m}$  in diameter. Another morphology which shows less corrosion due to a shorter immersion time can be seen in Fig. 3, which illustrates a slight pitting attack and the start of bubble formation. The formation of bubbles in these figures clearly shows gas build-up at the solid-melt interface. Previous investigators [8–10] observed this phenomenon and attributed it to the evolution of CO at the SiC/SiO<sub>2</sub> interface during the generated oxidation and corrosion on the SiC substrate. The present investigation proposes that  $V_2O_5$  is acting as a flux which carries a sufficient amount of oxygen from the heated air to enable the simple reaction:



This process is supported by two reasons: first, SiC will not be attacked by HF solution; the scales removed by HF are only SiO<sub>2</sub>. Secondly, the solubility between SiO<sub>2</sub> and the  $V_2O_5$  melt is negligible [7]. The reaction may be considered as follows: the oxygen enters into the  $V_2O_5$  flux, diffuses through the formed SiO<sub>2</sub> scale, reaches the interface of SiC/SiO<sub>2</sub>, reacts with solid SiC, and then the gases formed diffuse out of the scale. However, the entire mechanism has not been fully developed.



Figure 3 Slight pitting (bubbles start to form) on the surface of SiC after corrosion in the  $V_2O_5$  melt for 2 h at  $1000^\circ C$ .

Here, we start with the weight loss measurement in which corrosion products are measured over each time interval. The results of these corrosion treatments at four different temperatures are presented in Fig. 4. It is seen from the figure that increasing the temperature increases the corrosion rate of silicon carbide. The reaction rate indicates it should have a complex temperature dependence. If  $D_0$  is the diffusion coefficient of carbon monoxide and  $k_s$  is the rate constant at the solid surface, the rate can be written by

$$\frac{dW}{dt} = \frac{-CA}{b(W_0 - W)/D + k_s^{-1}} \quad (1)$$

Further, Equation 1 may be integrated to give the

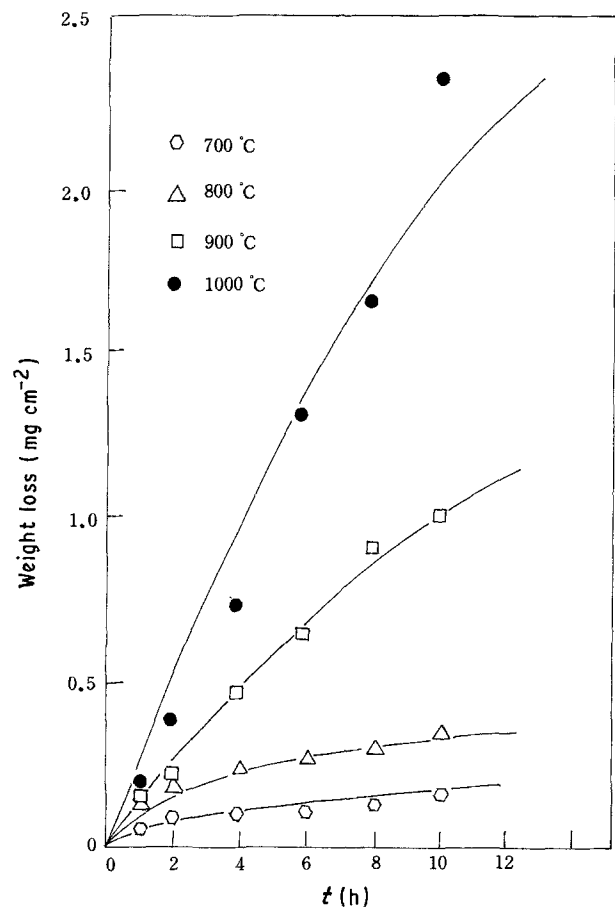


Figure 4 Weight loss of SiC in the  $V_2O_5$  melt.

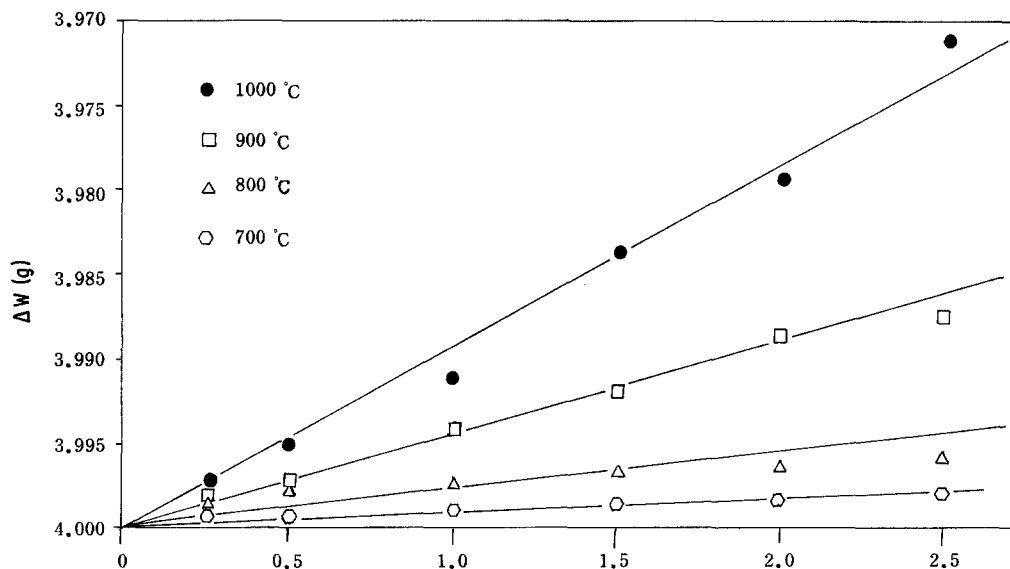


Figure 5 A data plot showing the correlation between the equations and linear kinetics.

expression:

$$t = \frac{b(\Delta W)^2}{2A_0CD} + \frac{\Delta W}{A_0Ck_s} \quad (2)$$

where  $A_0$  and  $C$  are the initial reaction area and initial concentration in the bulk respectively, and  $b$  is a constant factor. If  $W$  is the remaining weight per unit area at any reacting time  $t$ , the quantity  $\Delta W$  is then the difference between the initial weight of the unit area,  $W_0$ , and the value of  $W$ . It is known that both  $A_0$  and  $C$  remain unchanged during the reaction.

Equation 2 represents the sum of the parabolic and linear rates and is similar to the earlier developed equation by Wagner and Grunnewald [11, 12]. The  $\Delta W_0$  term in the equation can be divided resulting in the following:

$$\frac{t}{\Delta W} = K_D \Delta W + K_s \quad (3)$$

If we let

$$K_D = \frac{b}{2A_0CD} \quad K_s = \frac{1}{A_0Ck_s}$$

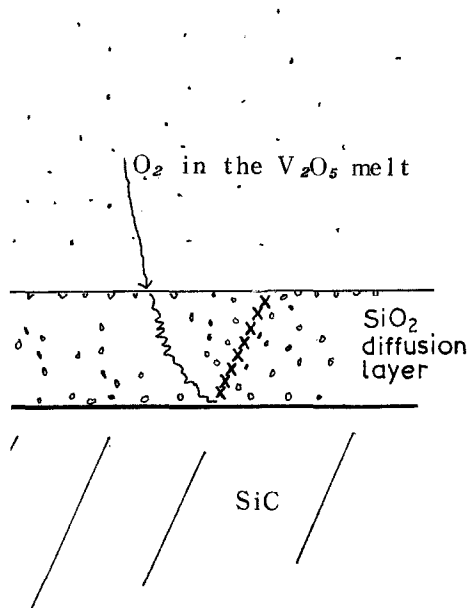


Figure 6 Schematic diagram of the hot corrosion mechanism.  $x$  represents the rate controlling step.

the equation predicts that  $t/\Delta W$  plotted against  $\Delta W$  should result in a straight line, the slope of which contains the rate constant due to the diffusion effect  $K_D$ . Figure 5 is plotted according to Equation 3 using the data from Fig. 4. The consistency of the linear relationship of the plotted data with the equation indicates that the above derivation is applicable to this study. It needs to be noted in Fig. 5 that the extrapolation of each straight line goes through the origin. This is because the diffusion coefficient  $D$  has a larger activation energy which is less sensitive to temperature change than the surface reaction constant  $k_s$ . Consequently at elevated temperatures  $k_s$  becomes much larger than  $D$ , so the reciprocal value  $K_s$  will be negligible. It is apparent from the equations that diffusion will be the rate controlling mechanism when hot corrosion behaviour occurs. These mathematical expressions correspond with the diagram shown in Fig. 6, and are able to explain the case of gas build-up in oxide scale on SiC. For instance, similar bubble formation has been observed by Mieskowski and colleagues [13], from which they also inferred that the rate of oxidation of SiC is controlled by the outward diffusion of CO. However, compared with other research, we would emphasize that here the severe corrosion of SiC in acidic  $V_2O_5$  melt occurred at much lower temperatures (less than  $1000^\circ\text{C}$ ). Therefore, a warning should be given regarding the use of oils containing  $V_2O_5$  in engines which incorporate components made from SiC.

#### 4. Conclusions

Silicon carbide is corroded in the hot acidic environment which is introduced by  $V_2O_5$  flux. A mathematical kinetic expression is determined for the entire hot corrosion behaviour. The consistency of the plotted data with the deduced equations has shown the excellence of the proposed mechanism. The surface reaction constant  $k_s$  is large enough for the chemical reaction to be negligible in the controlling kinetics. The outward diffusion of gas build-up inside the scales appears to be the rate determining step. The corrosion rate is determined and the resulting bubble formation is

attributed to the evolution of CO from the interface of SiC/SiO<sub>2</sub>. These observations suggest that careful protection of SiC engine components is required when using oils containing V<sub>2</sub>O<sub>5</sub>.

## References

1. J. I. FEDERER, *Adv. Ceram. Mater.* **3** (1988) 56.
2. J. L. SMIALEK and N. S. JACOBSON, *J. Amer. Ceram. Soc.* **69** (1986) 741.
3. N. S. JACOBSON and J. L. SMIALEK, *J. Amer. Ceram. Soc.* **68** (1985) 432.
4. D. W. McKEE and D. CHATTERJI, *J. Amer. Ceram. Soc.* **59** (1976) 441.
5. H. H. UHLIG and R. W. REVIE, in "Corrosion and Corrosion Control" (John Wiley, New York, 1984) p. 199.
6. Y. TAKEDA, T. KOSUGI, S. IJIMA and K. NAKAMURA, International Symposium on Ceramic Component for Engines (1983) p. 529.
7. E. M. LEVIN, C. R. ROBBINS and H. F. McMURDIE, in "Phase Diagrams for Ceramists" (The American Ceramic Society, Ohio, 1969) p. 110.
8. J. E. DOHERTY, *Proc. EMSA* **30** (1972) 538.
9. J. SCHLICHTING and J. KRIEGESMANN, *Ber. Dtsch. Keram. Ges.* **56** (1975) 72.
10. S. C. SINGHAL, *J. Mater. Sci.* **11** (1976) 1246.
11. M. E. WADSWORTH, *Trans. TMS/AIME* **245** (1969) 1381.
12. C. WAGNER and K. GRUNEWALD, *Z. Phys. Chem. (B)* **40** (1938) 455.
13. D. M. MIESKOWSKI, T. E. MICHELL and A. H. HEUER, *J. Amer. Ceram. Soc.* **67** (1984) C-17.

*Received 4 January  
and accepted 17 July 1989*